# Pion to two-photons transition form factor

M. Atif Sultan,[1, 2, *] Xianglong Song,[1, †] Lei Chang,[1, ‡] and Adnan Bashir[3, 4, §]

[1] *School of Physics, Nankai University, Tianjin 300071, China*
[2] *Centre For High Energy Physics, University of the Punjab, Lahore (54590), Pakistan*
[3] *Instituto de Física y Matemáticas, Universidad Michoacana de San Nicolás de Hidalgo, Morelia, Michoacán 58040, México*
[4] *Department of Integrated Sciences and Center for Advanced Studies in Physics, Mathematics and Computation, University of Huelva, E-21071 Huelva, Spain*

(Dated: April 1, 2024)

Based upon a combined formalism of Schwinger-Dyson and Bethe-Salpeter equations, we propose carefully constructed self-consistent models for the dressed quark propagator, for the Bethe-Salpeter amplitude of the pion and the electromagnetic quark-photon interaction vertex. We then compute the $\gamma^*\pi^0\gamma$ transition form factor $G^{\gamma^*\pi^0\gamma}(Q^2)$ for a wide range of photon momentum transfer squared $Q^2$. The quark propagator is expanded out in its perturbative functional form but with dynamically generated dressed quark mass. It has complex conjugate pole singularities in the complex-momentum plane which is motivated by the solution of the quark gap equation with rainbow-ladder truncations of the infinite set of Schwinger-Dyson equations. This complex pole singularity structure of the quark propagator can be associated with a signal of confinement which prevents quarks to become stable asymptotic states. The Bethe-Salpeter amplitude is expressed in terms of a spectral density function which is fully constrained by the distribution amplitude of the pion obtained from modern lattice data. The QCD evolution of the distribution amplitude is also incorporated into our model through the direct implementation of Efremov-Radyushkin-Brodsky-Lepage evolution equations. We incorporate the effects of the quark anomalous magnetic moment in the description of the quark-photon vertex whose infrared enhancement is known to dictate hadron properties. Once the model is constructed, we calculate the form factor $G^{\gamma^*\pi^0\gamma}(Q^2)$ and find it consistent with direct QCD-based studies and available experimental data. It slightly exceeds the conformal limit for large $Q^2$ which might be attributed to the lack of proper inclusion of the logarithmic QCD corrections to the ultraviolet limit. The associated interaction radius and neutral pion decay width turn out to be comparable with experimental data.

## I. INTRODUCTION

Quantum chromo dynamics (QCD) [1] is the theory of strong interaction in the Standard Model of the elementary particles. According to QCD the color charge is the fundamental property of the quarks and the gluons due to which they interact through strong interaction. QCD is a non-Abelian gauge theory which is renormalizable and exhibits asymptotic freedom [2, 3]. This feature allows us to study strong interaction processes using well established Feynman diagrammatic approach at energy scale greater than the QCD scale $\Lambda_{QCD}$. However at low energy, strong coupling is of order one or higher which makes the perturbation theory inapplicable. Therefore, at this energy scale one is forced to resort to less reliable and generally more difficult non-perturbative methods like lattice simulation of QCD [4], Dyson-Schwinger (DS) and Bethe-Salpeter (BS) approaches [5, 6].

All hadronic observables may be calculated if we know Green functions of QCD which satisfy a set of infinite, coupled, nonlinear integral equations which are the well-known Dyson-Schwinger equations (DSEs). In these equations the two-point one-particle irreducible (1PI) Green functions (propagators) are related to the three-point functions (vertices), which in turn are entangled with the four-point functions (scattering kernels), ad infinitum. It is a general formalism not limited to the perturbative domain. Before attempting any solution, this infinite set must be truncated by introducing mathematical model(s) of some suitable set of Green functions. That is why modelling remains a crucial component in hadron physics. However, despite this challenge, remarkable progress has been achieved in the non-pertubative QCD through the SDE-BSE approach, which has become an effective and decisive tool to study the strong interaction phenomena, for example, Refs. [7–12]. DSE-BSE approach have been extensively used to study the hadronic observables in vacuum and at a finite temperature.

Fortunately, our understanding of the intricate interplay between the quark propagator and the meson's BS Amplitude (BSA) [13] enables us to build their models that are amicable enough to allow for algebraic manipulations while still producing decent predictions of the physical observables. In this article, we carry out this algebraic model (AM) construction for pseudoscalar mesons. We model the momentum-dependent quark propagator, which captures complex conjugate singularities on the time-like half of the complex momentum plane related to the confinement. We also adopt the AM of BSA in

* atifsultan.chep@pu.edu.pk
† x.l.song@mail.nankai.edu.cn
‡ leichang@nankai.edu.cn
§ adnan.bashir@umich.mx

terms of the spectral density function (SDF) from Ref. [14]. The SDF can be written in terms of the distribution amplitude (DA), so that the need to specify SDF is completely circumvented with prior knowledge of the DA. The precise shape of the pion DA to be determined is an intriguing topic that has been studied using numerous approaches, e.g. the QCD sum rules, the Lattice QCD, the DSEs, etc. [14–18]. For DA, we use the lattice data to construct its model which has good chi-square fit with the data. DAs play an essential role in describing the various hard exclusive processes of QCD [19–21] such as pseudoscalar meson transition and electromagnetic form factors [19, 22], diffractive vector-meson production [23, 24] and also in the study of *CP*-violation via nonleptonic decays of heavy-light mesons [25, 26] etc.

More precise standard model (SM) prediction is needed to compare with forth-coming more-and-more precise experimental data, which will help to ensure whether there is new physics beyond the SM or not. The pion transition form factors (TFF) is a particularly significant component that is associated with the axial anomaly. The interaction of hadronic matter with two photons of arbitrary virtuality is described by meson TFF. Given that the chiral anomaly fixes the value of the pion TFF at the origin, which has made it a particularly interesting object of study while the behavior at large value of momentum ($Q^2$) has been predicted through perturbative QCD.

Till 1998, the CELLO [27] and CLEO [28] data were available for the pion TFF in the space-like region $Q^2 < 7\,GeV^2$. The *BABAR* collaboration [29] released data on the pion TFF for the space-like region $Q^2 \in [4, 40]$ around the end of 2009, and this data provoked a contentious debate by revealing the TFF's unexpected scaling violation. These results shows a rapid growth of $Q^2G^{\gamma^*\pi^0\gamma}(Q^2)$ for the region $Q^2 > 15$, which contradicts the well-known asymptotic prediction that $Q^2G^{\gamma^*\pi^0\gamma}(Q^2) \to$ constant for large $Q^2$. However the Belle collaboration measurements in 2012 for the same energy region contradict the *BABAR* data and showed that $Q^2G^{\gamma^*\pi^0\gamma}(Q^2) \to$ constant for large $Q^2$. Hopefully, the Belle II at SuperKEKB experiment [30] with less uncertainty could be helpful to clarify the above experimental discrepancies. The aim of this work is to reexamine these claims using an updated investigation of pion TFF with AM of the quark propagator, BSA and DA.

The article is organized as follows: in Sec.II, we briefly introduce the AM of the quark propagator, BSA, DA and its QCD evolution, and discuss the quark-photon vertex (QPV) with anomaluos magnetic moment term (AMM). In Sec. III, we discuss $\gamma^*\pi^0\gamma$ TFF in detail: in particular its connection with chiral anomaly, its asymptotic behavior in QCD and comparison with experimental data, the effect of AMM term on pion TFF and anomaly, and TFF related physical quantities. Finally, in Sec. IV, we present our conclusions and final remarks.

## II. FORMALISM

Bethe-Salpeter equation (BSE) [31, 32] provides the full relativistic depiction of meson bound states. These kind of bound states appear as poles for specific values of invariant masses in BSA and these masses depends on the quantum numbers of meson state. The BSE

$$[\Gamma_M(p;P)]_{tu} = \int \frac{d^4k}{(2\pi)^4} K^{rs}_{tu}(p,k;P) \times \Big(S_a(k_+)\Gamma_M(k;P)S_b(k_-)\Big)_{rs} \quad (1)$$

gives the BSA, 1-particle irreducible quark-meson vertex $\Gamma^{ab}_M(p;P)$, where $a$ and $b$ represent the flavor of quark and antiquark respectively, and $r$, $s$, $t$, $u$ represent collectively color and Dirac indices. Here $M$ specifies only the type of meson. The momentum conservation implies that $p_\pm = p \pm \eta_\pm P$ and $k_\pm = k \pm \eta_\pm P$ satisfying the condition $\eta_+ + \eta_- = 1$. The renormalized, amputated quark-antiquark kernel $K$ is irreducible with respect to cutting pair of quark-antiquark lines. The kernel $K$ furnish the physical input to BSE along with quark propagator and we must have it prior to achieve the solution for meson mass and BSA. For a comprehensive review of the DSE-BSE formalism and its applications to hadron physics, see Refs. [33–36].

The a-flavor dressed quark propagator $S_a$ is obtained as the solution of the quark DSE [34, 37–40]

$$S_a^{-1}(p) = (i\not{p}+m_a)+\frac{4}{3}g^2\int \frac{d^4k}{(2\pi)^4} D_{\mu\nu}(p-k)\gamma_\mu S_a(k)\Gamma_\nu(k,p). \quad (2)$$

Here $m_a$ is the a-flavor current quark mass and $g$ is the Lagrangian coupling constant. The rest of the ingredients of Eq. (2) are defined as usual: $D_{\mu\nu}$ and $\Gamma_\nu$, respectively, the fully dressed gluon propagator and quark-photon vertex (QPV), each of which satisfy their own DSE. In order to find solution we have to study their DSE too, which is a tough problem. However, such a study is beyond of the scope of this work. Despite this complication, many studies has been made to unveil their nonperturbative structure using their DSE [41–44], as well as lattice formulation [45–48]. In spite of the fact that propagators and BSA can be obtained from the corresponding DSEs and BSE solutions, more sensible, less complex models can yield useful and admissible insight [40, 49, 50].

### A. Modeling BSA, QPV and quark propagator

A simple model can be used to algebraically elucidate the important features before using the numerical solution of the propagator and BSA. We work in the chiral limit and suppose the quark propagator taking the following simple momentum dependent form

$$S^{-1}(k) = i\gamma\cdot k + B(k^2)\,, \quad (3)$$

with the quark mass function as [51]

$$B(k^2) = \frac{M^3}{k^2 + M^2}\,, \tag{4}$$

here $M$ is mass for a given quark flavor. An advanced form of Eq. (4) is that one can write the quark propagator by the following form

$$S(k) = \sum_{j=1}^{3} \frac{-i\gamma\cdot k\alpha_j + \beta_j M}{k^2 + \gamma_j M^2}\,, \tag{5}$$

where $\alpha_j$, $\beta_j$ and $\gamma_j$ taking the following values

$$\begin{aligned}
\alpha_j &= \{0.411 + 0.276i, 0.411 - 0.276i, 0.177\}\,,\\
\beta_j &= \{0.117 + 0.414i, 0.117 - 0.414i, -0.234\}\,,\\
\gamma_j &= \{0.123 + 0.745i, 0.123 - 0.745i, 1.754\}\,.
\end{aligned}$$

It has long been known that the rainbow-Ladder (RL) truncation to the quark propagator DSE produces complex conjugate singularities on the time-like half of the complex momentum plane which some how is related to the confinement. Our present model of quark propagator can catch these singularities which would play an essential role in this work. In practice $M = 0.505521GeV$ to produce pion decay constant as $0.0924GeV$.

The pion's momentum dependent form of BSA is [14]

$$\Gamma(k;P) = i\gamma_5 \frac{M}{f_\pi}\int_{-1}^{1} \rho(z)\frac{M^2}{(k + z\frac{P}{2})^2 + M^2}\,\mathrm{d}z, \tag{6}$$

where $P^2 = -m_\pi^2$ and $M$ is fixed such that $f_\pi = 0.0924GeV$. The $\rho(z)$ is a SDF whose precise shape determines the pointwise behavior of the meson's BSA. At $P = 0$, i.e., soft pion limit, we get the exact relation

$$\Gamma(k;P=0) = i\gamma_5\frac{B(k^2)}{f_\pi}, \tag{7}$$

where $B(k^2)$ is the Lorentz scalar function appearing in the quark inverse propagator.

The QPV ansatz is given by

$$\Gamma_\mu(Q) = \gamma_\mu + \frac{\sigma_{\mu\nu}Q_\nu}{M}V(Q^2), \tag{8}$$

where $V(Q^2)$ can be regarded as a profile function for an an anomalous magnetic moment (AMM) term, and

$$V(Q^2) = \frac{C_0 M^2\hat{\xi}}{\mathcal{K}(C_0^2M^2\hat{\xi} + 2\bar{C}_0\mathcal{I}) - \mathcal{I}}, \tag{9}$$

where the integrals:

$$\begin{aligned}
C_\alpha(Q^2) &= \int_0^1 I_\alpha(\omega(M^2,u,Q^2))du,\\
\bar{C}_\alpha(Q^2) &= \int_0^1 u(u-1)I_\alpha(\omega(M^2,u,Q^2))du,
\end{aligned} \tag{10}$$

with $\mathcal{I} = 1 - \hat{\xi}(2C_0M^2 + C_2)$, $\mathcal{K} = \frac{8Q^2}{3m_G^2}$ and $\hat{\xi} = \frac{32\xi}{9m_G^2}$. Note that QPV is independent of the relative momentum of the quark and antiquark, and thus depends only on the photon momentum $Q$.

It is worth noting that the dressing function $V(Q^2)$ of AMM term is proportional to strength parameter $\xi$, which is why AMM term disappears in $\xi = 0$ limit and $V(Q^2) \to 0$ as $Q^2 \to \infty$. Finally, it is appropriate to display the value of the dressing function at $Q^2 = 0$

$$V(0) = \frac{\hat{\xi}M^2 I_0(M^2)}{1 - \hat{\xi}(2M^2I_0(M^2) + I_2(M^2))}. \tag{11}$$

Thus, as we shall discuss in section III, the AMM term could indeed contribute to the chiral anomaly in $\gamma^*\pi^0\gamma$ TFF quantitatively. Some details of the QPV dressing function can be found in Refs. [52, 53].

### B. The QCD evolution of the pion distribution amplitude

The QCD evolution of the distribution amplitude (DA) is specified by the Efremov-Radyushkin-Brodsky-Lepage (ERBL) equations, derived in Refs. [19, 22, 54]. This completely determine the logarithmic dependency of the DAs on $\xi$. At the leading order, the QCD evolution equations for the DAs can be expressed in terms of Gegenbauer polynomials [55]

$$\phi(x,\xi) = x(1-x)\sum_{n=0}^{\infty} a_n C_n^{3/2}(2x-1)\left(\ln\frac{\xi^2}{\Lambda^2}\right)^{-\gamma_n}, \tag{12}$$

where only even $n$ contribute, and the anomalous dimensions are

$$\gamma_n = \frac{C_F}{\beta}\left(1 + 4\sum_{2}^{n+1}\frac{1}{k} - \frac{2}{(n+1)(n+2)}\right), \tag{13}$$

where $C_F = \frac{Nc^2-1}{2Nc}$ and $\beta = \frac{11}{3}N_c - 2/3N_f$. Once the coefficients $a_n$ are determined, the evolution equation would be completely known. These coefficients can be calculated using the initial conditions that the model calculation provides. By using initial distribution $\phi(x_i,\xi_0)$ along with the Gegenbauer polynomials orthogonality relation,

$$a_n\left(\ln\frac{\xi_0^2}{\Lambda_Q^2 CD}\right)^{-\gamma_n} = 4\frac{2n+3}{(n+1)(n+2)}\int_0^1 \mathrm{d}x C_n^{3/2}(2x-1)\phi(x,\xi_0), \tag{14}$$

with $\Lambda_Q CD = 0.234\,GeV$ being the QCD scale parameter. one might be able to find the $a_n$ coefficients to determined the evolution equations. All model calculations should be consistent with the theoretical asymptotic behavior of DA after evolution.

The pion TFF is sensitive to the shape of the pion DA. The precise behavior of the pion DA is an intriguing issue

that has been explored using numerous approaches, e.g. the QCD sum rules, the Lattice QCD, the DSEs, and etc. [14, 17, 56–59]. Most of these favors the asymptotic form proposed by Lepage and Brodsky [19]. In this paper, We consider the following expression for the pion DA

$$\phi(x) = \mathcal{N}\frac{\log(1+Ax(1-x))}{B}, \tag{15}$$

where $\mathcal{N}$ is fixed such that $\int_0^1 \mathrm{d}x\phi(x) = 1$. The best fitted values of parameters with lattice data are:

$$A = 479.57, B = 3.97158.$$

The pion DA in Eq.(15) is fitted with latest available lQCD calculations data quoted at $\xi_2 = \xi = 2GeV$ in Ref. [60]. We therefore employ leading-order QCD evolution Eq. (12) to obtain the $\phi(x,\xi_3)$ at $\xi_3 = \xi = 3GeV$. We used $\phi(x,\xi_3)$ for the calculation of pion spectral density at this scale, and the procedure of finding the pion spectral density from the DA can be found in the appendix of Ref. [50].

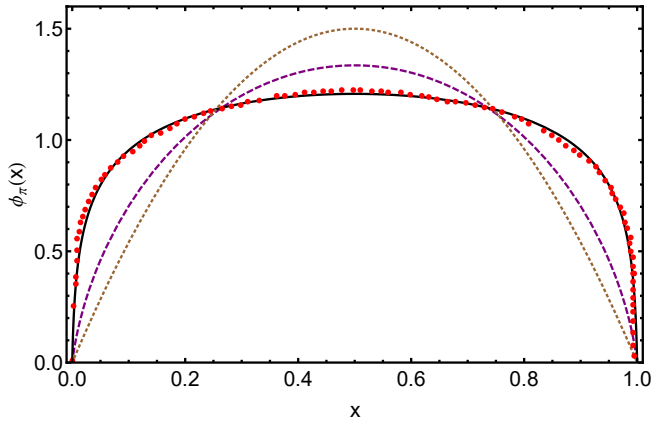


FIG. 1. DAs for $\pi$. *Black solid curve*—pion DA in Eq. (15); *Red disks*—the data reported in Ref.[60]; *Purple dashed curve*—evolved pion DA at hadronic scale $\xi_3 = \xi = 3GeV$; *Brown dotted curve*—the asymptotic DA $\phi_{asy}(x) = 6x(1-x)$.

We depict the pion DAs in Fig. 1, and compare them with the asymptotic two-particle distribution $\phi_{asy}(x) = 6x(1-x)$, and also with a lattice simulation data. Due to the dominance of dynamical chiral symmetry breaking (DCSB), $\phi_{\xi=2GeV}(x)$ is broader than $\phi_{asy}(x)$. $\phi_{\xi=3GeV}(x)$ is close to $\phi_{asy}(x)$ but is also dilated. All the DAs are symmetrical in Fig. 1.

## III. TRANSITION FORM FACTOR: $\gamma^*\pi^0\gamma$

A single scalar function describe the transition $\gamma^*\gamma \to \pi^0$, required to fully express the amplitude:

$$T_{\mu\nu}(k_1,k_2) = \frac{e^2}{4\pi^2 f_\pi}\epsilon_{\mu\nu k_1 k_2} G(k_1^2, k_1\cdot k_2, k_2^2), \tag{16}$$

where $k_1$ and $k_2$ are the photon momenta. The general impulse approximation for the transition amplitude of $\gamma^*\gamma \to \pi^0$ can be expressed as [53, 61, 62]

$$T_{\mu\nu}(k_1,k_2) = \frac{N_c}{3} tr \int_q i\Gamma_\nu(k_2)S(q-k_2) \times \Gamma_\pi(P)S(q+k_1)i\Gamma_\mu(k_1)S(q), \tag{17}$$

where $P = -k_1 - k_2$ is the total momentum of pion meson, such that $P^2 = m_\pi^2$. The kinematic constraints are

$$k_1^2 = Q^2,\ k_2^2 = 0,\ k_1\cdot k_2 = -(Q^2+m_\pi^2)/2. \tag{18}$$

By incorporating these kinematic constraints, the pion TFF is defined as

$$G^{\gamma^*\pi^0\gamma}(Q^2) = 2G(Q^2, -(Q^2+m_\pi^2)/2, 0), \tag{19}$$

where the factor 2 appears in order to account for the possible ordering of the photons. The other elements in Eq. (17) are the quark propagator, pion BSA and the dressed QPV determined in the previous section. It is in principle straightforward to compute this transition. The isospin symmetry approximation, which assumes that up (u) and down (d) quarks have identical strong interactions other than electric charge, is used.

We first consider the chiral limit and $Q^2 = 0$, in which case one must calculate chiral anomaly *i.e.* $G(0,0,0)$ using Eq. 17. The first thing to note is that only bare vertex *i.e.* $\xi = 0$ fails to produce the chiral anomaly. Focusing on the dressed QPV, it reveals that the AMM term indeed contribute the chiral anomaly. To address this observation, let us consider $\xi = 0$ limit and calculate Eq. 17. In this limit, $G^{\xi=0}(0,0,0) \neq \frac{1}{2}$. Thus the value specified by the chiral anomaly is not met. So we fix the value of strength parameter $\xi$ to acquire $G(0,0,0) = \frac{1}{2}$. Within our choice of models of the quark propagator, QPV, BSA and the pion DA we find that the chiral anomaly $G^{\xi=0.21645}(0,0,0) = \frac{1}{2}$.

Our calculation result of $\gamma^*\pi^0\gamma$ TFF is depicted in Fig. 2. It is clear that $G^{\gamma^*\pi^0\gamma}(Q^2)$ is decreasing function of $Q^2$. It decreases rapidly for small values of $Q^2$, while decreases slowly for large values of $Q^2$. It is also evident that our results agree with the experimental data for all the range of $Q^2$, where results are available, and the results reported in Refs. [61, 63]. Moreover, $G^{\gamma^*\pi^0\gamma}(Q^2)$ behaves like $1/Q^2$ for large $Q^2$. Our numerical results suggest that the form factor is a nearly monopole and can be satisfactorily simulated by a vector meson dominance (VMD) formula $F(Q^2) = m_\rho^2/(m_\rho^2+Q^2)$. Lepage and Brodsky [19] showed that TFF behaves like $Q^2F(Q^2) \to 8\pi^2 f_\pi^2 = 0.674GeV^2$ in the asymptotic region while Fig. 2 suggests slightly higher asymptotic mass scale.

Our $\gamma^*\pi^0\gamma$ TFF for one real and one virtual photon for the large $Q^2$ behavior is shown in Fig. 3, together with the experimental results. We preset two curves, one where we evolve pion DA at hadronic scale $\phi(x,\xi_3)$ and

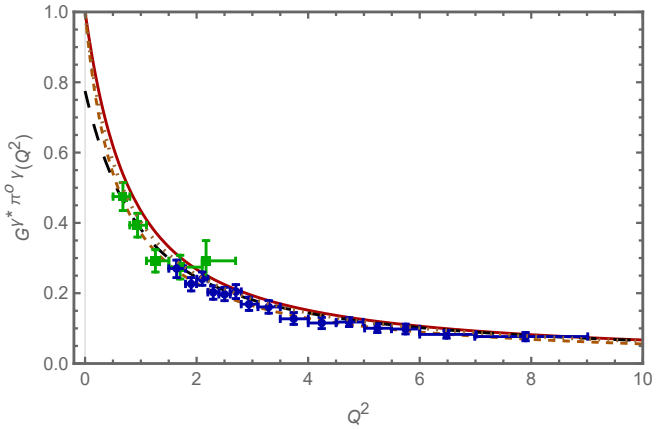


FIG. 2. $\gamma^*\pi^0\gamma$ transition form factor. *Red solid curve*—computation with Eq. (16) using dressed vertex; *Black long-dashed curve*—computation with Eq. (16) using bare vertex; *Orange dashed curve*—VMD monopole result with mass scale $m_\rho^2 = 0.59 GeV^2$; *Brown dotted curve*—corresponds to a monopole fit to the QCD-based result in Ref. [61], which agrees with the data reported in Refs. [27, 28], green squares and blue disks, respectively.

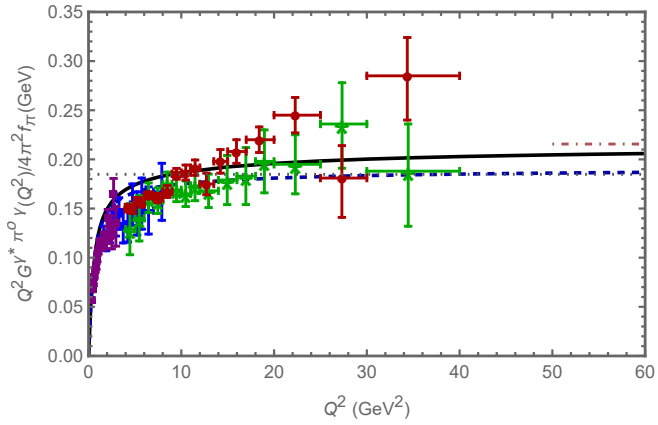


FIG. 3. $Q^2$-weighted $\gamma^*\pi^0\gamma$ transition form factor. Curves: *Black solid curve*—$Q^2 G^{\gamma^*\pi^0\gamma}(Q^2)$ obtained from Eq. (16) using evolved DA at $\xi_3$; *Blue dashed curve*—result obtained from Eq. (16) using asymptotic DA $\phi_{asy}(x)$; *Gray dotted curve*—the limit with asymptotic PDA input; *Pink dot-dashed curve*—related to the limit with the present model PDA input; Data: BESIII (preliminary) [75]—Squares (Purple); CLEO [28]—Diamonds (Blue); Belle [28]—Stars (Green); *BABAR* [29]—Disks (Red).

one where we use the $\phi_{asy}(x)$ . Our prediction is indicated by the solid (black) curve. The asymptotic value of $\pi^0$ TFF is $2f_\pi = 0.185 GeV$, drawn as the dotted (gray) curve. From Figs. 2 and 3 we can see that pion TFF is in agreement with perturbative QCD which predicts constant behavior of Pion TFF at very large $Q^2$. In the range $Q^2 \leq 3\,GeV^2$, pion TFF agrees with the available BESIII (preliminary) data, and have the same behavior as experimental determination, within the error bars, in $2\,GeV^2 \leq Q^2 \leq 8\,GeV^2$ region. Fig. 3 shows that Pion TFF has sharper $Q^2$ dependence in the range $Q^2 \leq 14\,GeV^2$ than the experimental measurements, and has good agreement with Belle Collaborations beyond this range. The increase found by the *BABAR* Collaboration for $Q^2 \geq 10\,GeV^2$ is not reproduced. In addition, there are theoretical studies claiming that *BABAR* data is not compatible with QCD calculations [64–67]. It is also shown in Ref. [68] that the *BABAR* data behavior at large $Q^2$ can not be explained with QCD calculations by using the asymptotic QCD, AdS/QCD, and Chernyak-Zhitnitsky models for the DA but can be supported by a flat modeling of the pion DA model [68, 69] which underestimate significantly the pion TFF at low $Q^2$. On the other hand, there are also phenomenological studies that support the *BABAR* findings [70–74].

Within the large $Q^2$ limit, the analytical expression can be obtained within this model as follows [51]:

$$\frac{1}{4\pi^2 f_\pi} Q^2 G^{\gamma^*\pi^0\gamma}(Q^2 \to \infty) = 8 f_\pi \int_{-1}^{1} \mathrm{d}w \frac{\log(\frac{1+w}{2})}{3(w-1)} \rho(w) = 2 f_\pi \int_0^1 \mathrm{d}x \frac{\phi(x)}{3(1-x)}, \quad (20)$$

which is consistent to the QCD predication with the input of DA related to $\rho(w)$. Fig. 3 shows that the TFF increases as $Q^2$ increases and overtakes the perturbative prediction limit $2f_\pi$. At very large value of $Q^2$, the TFF goes to the limit $\frac{7}{6} 2 f_\pi$ from below.

For on-shell photons, we also calculated the neutral pion decay width and the corresponding interaction radius. Pion's interaction radius is defined as

$$r_{\pi^0}^2 = -6 \frac{d}{dQ^2} \ln g_{\pi\gamma\gamma}(Q^2)|_{Q^2=0}, \quad (21)$$

where $g_{\pi\gamma\gamma}(Q^2) = G^{\xi=0.21645}(Q^2, -(Q^2+m_\pi^2)/2, 0)$. Our computed interaction-radius is $r_{\pi^0} = 0.52\,\mathrm{fm}$, which is approximately 20% less than the experimental value $r_{\pi^0} = 0.65 \pm 0.03\,\mathrm{fm}$ [27]. Whereas in the limit $\xi = 0$, $r_{\pi^0} = 0.46\,\mathrm{fm}$ which is more less than experimental estimate. This implies that the presence of the AMM term in QPV is crucial.

For completeness, we have also calculated the corresponding decay width, viz.,

$$\Gamma_{\pi^0\gamma\gamma} = \frac{g_{\pi\gamma\gamma}^2(Q^2) \alpha_{em}^2 m_\pi^3}{16\pi^3 f_\pi^2}|_{Q^2=0}, \quad (22)$$

where $\alpha_{em} = 1/137$ is fine-structure constant. The decay width produced by Eq.22 is $\Gamma = 8.02\,\mathrm{eV}$, which is a good agreement with the experimental value $\Gamma = 7.82 \pm 0.14 \pm 0.17\,\mathrm{eV}$ [76]. Since the decay width is very sensitive to the pion mass , we use the experimental mass $m_\pi = 134.9768 \pm 0.0005\,\mathrm{MeV}$ [76].

## IV. CONCLUSION

In this work we have computed the pion TFF, $G^{\gamma^*\pi^0\gamma}(Q^2)$, for one real and one virtual photon in which models of the quark propagator, pion BSA and the QPV are used instead of the solutions of their corresponding QCD's DSE. For completeness, we also have calculated the pion interaction radius and the corresponding decay width. We model the momentum dependent quark propagator that capture the complex conjugate singularities on the complex momentum plane which is related to the confinement. In doing so we model the pion DA which have best fit to the Lattice data, and then evolve it according to the ERBL evolution equation from perturbative QCD at hadronic scale and find the corresponding spectral density to complete the calculations of the pion TFF. The calculations based upon the bare vertex and the dressed QPV, by adding the quark AMM term to tree level vertex. While both ansatz of QPV produces the same qualitative behavior of the pion TFF. The quark AMM term would play an essential role to produce the correct chiral anomaly.

Let's first recall that the tree level vertex fails to produce the chiral anomaly, which is associated with on-shell photon and chiral limit pion, *i.e.* $G(0,0,0)$. However the AMM term could be adequately regarded as an effective term that contributes to normalize the form factor. So the strength parameter $\xi$ can be tuned to produce chiral anomaly, *i.e.* $G(0,0,0) = \frac{1}{2}$. It is worth noticing that the dressed QPV follows the asymptotic limit , *i.e.* $\Gamma_\mu(Q) \to \gamma_\mu$ as $Q^2 \to \infty$. It is clear from Fig. 2 that the AMM term strengthen the QPV in low $Q^2$ domain, and its contribution disappears as $Q^2$ increases. In this case, the values for the interaction radius and decay width are consistent with the empirical findings.

Our pion TFF result using the evolved pion DA is in agreement with experimental data, and have sharp $Q^2$ dependance around $Q^2 = 10\,GeV^2$, but disagrees with the rapid increase in large $Q^2$ region suggested by *BABAR* collaboration and have reasonable agreement with Belle data. The computation at any desired value of spacelike $Q^2$ is an extra advantage of algebraic model due to its simplicity. We also find that our numerical result for the pion TFF agrees well with BESIII (preliminary) data in the domain $Q^2 \leq 3\,GeV^2$. It is hoped that the upcoming, more precise results from the Belle II experiment would help to explain the previous discrepancies between experimental observations and theoretical predictions [30].

In conclusion, we suggest a model of pion DA which is simple but offers a powerful tool for the analysis of the parton distribution and electromagnetic properties, and the momentum-dependent model of the quark propagator which capture confinement related complex conjugate singularities. We also like to point out that the improvement in BSA like evolution with running scale would be necessary.

## ACKNOWLEDGMENTS

Work supported by National Natural Science Foundation of China (grant no. 12135007).

[1] H. Fritzsch, M. Gell-Mann, and H. Leutwyler, Advantages of the Color Octet Gluon Picture, Phys. Lett. B **47**, 365 (1973).
[2] D. J. Gross and F. Wilczek, Ultraviolet Behavior of Nonabelian Gauge Theories, Phys. Rev. Lett. **30**, 1343 (1973).
[3] H. D. Politzer, Reliable Perturbative Results for Strong Interactions?, Phys. Rev. Lett. **30**, 1346 (1973).
[4] K. G. Wilson, Confinement of quarks, Physical review D **10**, 2445 (1974).
[5] F. J. Dyson, The Radiation theories of Tomonaga, Schwinger, and Feynman, Phys. Rev. **75**, 486 (1949).
[6] J. S. Schwinger, On the Green's functions of quantized fields. 1., Proc. Nat. Acad. Sci. **37**, 452 (1951).
[7] C. D. Roberts and A. G. Williams, Dyson-Schwinger equations and their application to hadronic physics, Prog. Part. Nucl. Phys. **33**, 477 (1994), arXiv:hep-ph/9403224.
[8] R. Alkofer and L. von Smekal, The Infrared behavior of QCD Green's functions: Confinement dynamical symmetry breaking, and hadrons as relativistic bound states, Phys. Rept. **353**, 281 (2001), arXiv:hep-ph/0007355.
[9] P. Maris and C. D. Roberts, Dyson-Schwinger equations: A Tool for hadron physics, Int. J. Mod. Phys. E **12**, 297 (2003), arXiv:nucl-th/0301049.
[10] A. Bashir, L. Chang, I. C. Cloet, B. El-Bennich, Y.-X. Liu, C. D. Roberts, and P. C. Tandy, Collective perspective on advances in Dyson-Schwinger Equation QCD, Commun. Theor. Phys. **58**, 79 (2012), arXiv:1201.3366 [nucl-th].
[11] C. S. Fischer, QCD at finite temperature and chemical potential from Dyson–Schwinger equations, Prog. Part. Nucl. Phys. **105**, 1 (2019), arXiv:1810.12938 [hep-ph].
[12] M. A. Sultan, F. Akram, B. Masud, and K. Raya, Effect of the quark-gluon vertex on dynamical chiral symmetry breaking, Phys. Rev. D **103**, 054036 (2021), arXiv:1810.01396 [nucl-th].
[13] D. Binosi, L. Chang, J. Papavassiliou, S.-X. Qin, and C. D. Roberts, Symmetry preserving truncations of the gap and Bethe-Salpeter equations, Phys. Rev. D **93**, 096010 (2016), arXiv:1601.05441 [nucl-th].
[14] L. Chang, I. Cloet, J. Cobos-Martinez, C. Roberts, S. Schmidt, and P. Tandy, Imaging dynamical chiral-symmetry breaking: pion wave function on the light front, Physical review letters **110**, 132001 (2013).
[15] S. J. Brodsky and G. F. de Teramond, Light-Front Dynamics and AdS/QCD Correspondence: The Pion Form Factor in the Space- and Time-Like Regions, Phys. Rev.

D **77**, 056007 (2008), arXiv:0707.3859 [hep-ph].
[16] G. S. Bali, V. M. Braun, S. Bürger, M. Göckeler, M. Gruber, F. Hutzler, P. Korcyl, A. Schäfer, A. Sternbeck, and P. Wein (RQCD), Light-cone distribution amplitudes of pseudoscalar mesons from lattice QCD, JHEP **08**, 065, [Addendum: JHEP 11, 037 (2020)], arXiv:1903.08038 [hep-lat].
[17] Z.-F. Cui, M. Ding, F. Gao, K. Raya, D. Binosi, L. Chang, C. D. Roberts, J. Rodríguez-Quintero, and S. M. Schmidt, Kaon and pion parton distributions, The European Physical Journal C **80**, 1 (2020).
[18] N. G. Stefanis, Pion-photon transition form factor in light cone sum rules and tests of asymptotics, Phys. Rev. D **102**, 034022 (2020), arXiv:2006.10576 [hep-ph].
[19] G. P. Lepage and S. J. Brodsky, Exclusive processes in perturbative quantum chromodynamics, Physical Review D **22**, 2157 (1980).
[20] V. L. Chernyak and A. R. Zhitnitsky, Asymptotic Behavior of Exclusive Processes in QCD, Phys. Rept. **112**, 173 (1984).
[21] S. J. Brodsky and G. P. Lepage, Exclusive Processes in Quantum Chromodynamics, Adv. Ser. Direct. High Energy Phys. **5**, 93 (1989).
[22] G. P. Lepage and S. J. Brodsky, Exclusive processes in quantum chromodynamics: Evolution equations for hadronic wavefunctions and the form factors of mesons, Physics Letters B **87**, 359 (1979).
[23] J. R. Forshaw and R. Sandapen, An AdS/QCD holographic wavefunction for the rho meson and diffractive rho meson electroproduction, Phys. Rev. Lett. **109**, 081601 (2012), arXiv:1203.6088 [hep-ph].
[24] F. Gao, L. Chang, Y.-X. Liu, C. D. Roberts, and S. M. Schmidt, Parton distribution amplitudes of light vector mesons, Phys. Rev. D **90**, 014011 (2014), arXiv:1405.0289 [nucl-th].
[25] B. El-Bennich, A. Furman, R. Kaminski, L. Lesniak, B. Loiseau, and B. Moussallam, CP violation and kaon-pion interactions in B —> K pi+ pi- decays, Phys. Rev. D **79**, 094005 (2009), [Erratum: Phys.Rev.D 83, 039903 (2011)], arXiv:0902.3645 [hep-ph].
[26] C. Shi, C. Chen, L. Chang, C. D. Roberts, S. M. Schmidt, and H.-S. Zong, Kaon and pion parton distribution amplitudes to twist-three, Phys. Rev. D **92**, 014035 (2015), arXiv:1504.00689 [nucl-th].
[27] H. J. Behrend *et al.* (CELLO), A Measurement of the pi0, eta and eta-prime electromagnetic form-factors, Z. Phys. C **49**, 401 (1991).
[28] J. Gronberg, T. Hill, R. Kutschke, D. Lange, S. Menary, R. Morrison, H. Nelson, T. Nelson, C. Qiao, J. Richman, *et al.*, Measurements of the meson-photon transition form factors of light pseudoscalar mesons at large momentum transfer, Physical Review D **57**, 33 (1998).
[29] B. Aubert, Y. Karyotakis, J. Lees, V. Poireau, E. Prencipe, X. Prudent, V. Tisserand, J. G. Tico, E. Grauges, M. Martinelli, *et al.*, Measurement of the $\gamma\,\gamma^* \to \pi\,0$ transition form factor, Physical Review D **80**, 052002 (2009).
[30] W. Altmannshofer *et al.* (Belle-II), The Belle II Physics Book, PTEP **2019**, 123C01 (2019), [Erratum: PTEP 2020, 029201 (2020)], arXiv:1808.10567 [hep-ex].
[31] E. E. Salpeter and H. A. Bethe, A relativistic equation for bound-state problems, Physical Review **84**, 1232 (1951).
[32] M. Gell-Mann and F. Low, Bound states in quantum field theory, Physical Review **84**, 350 (1951).
[33] C. D. Roberts and A. G. Williams, Dyson-schwinger equations and their application to hadronic physics, Progress in Particle and Nuclear Physics **33**, 477 (1994).
[34] R. Alkofer and L. Von Smekal, The infrared behaviour of qcd green's functions: confinement, dynamical symmetry breaking, and hadrons as relativistic bound states, Physics Reports **353**, 281 (2001).
[35] A. Bashir, L. Chang, I. C. Cloet, B. El-Bennich, Y.-X. Liu, C. D. Roberts, and P. C. Tandy, Collective perspective on advances in dyson—schwinger equation qcd, Communications in theoretical physics **58**, 79 (2012).
[36] I. G. Aznauryan, A. Bashir, V. M. Braun, S. J. Brodsky, V. D. Burkert, L. Chang, C. Chen, B. El-Bennich, I. C. Cloet, P. L. Cole, *et al.*, Studies of nucleon resonance structure in exclusive meson electroproduction, International Journal of Modern Physics E **22**, 1330015 (2013).
[37] P. Maris and C. D. Roberts, Dyson–schwinger equations: a tool for hadron physics, International Journal of Modern Physics E **12**, 297 (2003).
[38] A. Höll, C. Roberts, and S. Wright, Hadron physics and dyson-schwinger equations, arXiv preprint nucl-th/0601071 (2006).
[39] C. D. Roberts, M. Bhagwat, A. Höll, and S. Wright, Aspects of hadron physics, The European Physical Journal Special Topics **140**, 53 (2007).
[40] M. A. Sultan, K. Raya, F. Akram, A. Bashir, and B. Masud, Effect of the quark-gluon vertex on dynamical chiral symmetry breaking, Physical Review D **103**, 054036 (2021).
[41] R. Alkofer, W. Detmold, C. Fischer, and P. Maris, Analytic properties of the landau gauge gluon and quark propagators, Physical Review D **70**, 014014 (2004).
[42] R. Alkofer, W. Detmold, C. Fischer, and P. Maris, Analytic structure of the gluon and quark propagators in landau gauge qcd, Nuclear Physics B-Proceedings Supplements **141**, 122 (2005).
[43] R. Alkofer, C. S. Fischer, F. J. Llanes-Estrada, and K. Schwenzer, The quark–gluon vertex in landau gauge qcd: Its role in dynamical chiral symmetry breaking and quark confinement, Annals of Physics **324**, 106 (2009).
[44] C. S. Fischer, Non-perturbative propagators, running coupling and dynamical mass generation in ghost-antighost symmetric gauges in qcd, arXiv preprint hep-ph/0304233 (2003).
[45] A. Cucchieri and T. Mendes, What´ s up with ir gluon and ghost propagators in landau gauge? a puzzling answer form huge lattices, Proceedings of Science , 1 (2007).
[46] J. Skullerud, P. O. Bowman, A. Kizilersü, D. B. Leinweber, and A. G. Williams, Nonperturbative structure of the quark-gluon vertex, Journal of High Energy Physics **2003**, 047 (2003).
[47] J. Skullerud and A. Kizilersü, Quark-gluon vertex from lattice qcd, Journal of High Energy Physics **2002**, 013 (2002).
[48] J.-I. Skullerud, P. O. Bowman, A. Kizilersu, D. B. Leinweber, and A. G. Williams, Quark-gluon vertex in arbitrary kinematics, arXiv preprint hep-lat/0408032 (2004).
[49] L. Chang, C. Mezrag, H. Moutarde, C. D. Roberts, J. Rodríguez-Quintero, and P. C. Tandy, Basic features of the pion valence-quark distribution function, Physics Letters B **737**, 23 (2014).
[50] L. Albino, I. Higuera-Angulo, K. Raya, and A. Bashir, Pseudoscalar mesons: Light front wave functions, gpds, and pdfs, Physical Review D **106**, 034003 (2022).

[51] L. Chang, A perspective on dyson-schwinger equation: toy model of pion, in *EPJ Web of Conferences*, Vol. 113 (EDP Sciences, 2016) p. 05001.

[52] Z. Xing, K. Raya, and L. Chang, Quark anomalous magnetic moment and its effects on the $\rho$ meson properties, Physical Review D **104**, 054038 (2021).

[53] H. Dang, Z. Xing, M. A. Sultan, K. Raya, and L. Chang, The chiral anomaly and the pion transition form factor: beyond the cutoff, arXiv preprint arXiv:2306.04307 (2023).

[54] S. J. Brodsky and G. P. Lepage, *Exclusive processes and the exclusive-inclusive connection in quantum chromodynamics*, Tech. Rep. (SLAC National Accelerator Lab., Menlo Park, CA (United States); Cornell Univ ..., 1979).

[55] A. Courtoy, Generalized parton distributions of pions. spin structure of hadrons, arXiv preprint arXiv:1010.2974 (2010).

[56] S. J. Brodsky and G. F. de Teramond, Light-front dynamics and ads/qcd correspondence: the pion form factor in the space-and time-like regions, Physical Review D **77**, 056007 (2008).

[57] S. Mikhailov, A. Pimikov, and N. Stefanis, Systematic estimation of theoretical uncertainties in the calculation of the pion-photon transition form factor using light-cone sum rules, Physical Review D **93**, 114018 (2016).

[58] N. Stefanis, Pion-photon transition form factor in light cone sum rules and tests of asymptotics, Physical Review D **102**, 034022 (2020).

[59] X. Gao, A. D. Hanlon, N. Karthik, S. Mukherjee, P. Petreczky, P. Scior, S. Syritsyn, and Y. Zhao, Pion distribution amplitude at the physical point using the leading-twist expansion of the quasi-distribution-amplitude matrix element, Physical Review D **106**, 074505 (2022).

[60] J. Hua, M.-H. Chu, F.-C. He, J.-C. He, X. Ji, A. Schäfer, Y. Su, P. Sun, W. Wang, J. Xu, *et al.*, Pion and kaon distribution amplitudes from lattice qcd, Physical Review Letters **129**, 132001 (2022).

[61] P. Maris and P. C. Tandy, Electromagnetic transition form factors of light mesons, Physical Review C **65**, 045211 (2002).

[62] K. Raya, L. Chang, A. Bashir, J. J. Cobos-Martinez, L. X. Gutiérrez-Guerrero, C. D. Roberts, and P. C. Tandy, Structure of the neutral pion and its electromagnetic transition form factor, Physical Review D **93**, 074017 (2016).

[63] J. Chen, M. Ding, L. Chang, and Y.-x. Liu, Two-photon transition form factor of $c^- c$ quarkonia, Physical Review D **95**, 016010 (2017).

[64] H. Roberts, C. Roberts, A. Bashir, L. Gutiérrez-Guerrero, and P. Tandy, Abelian anomaly and neutral pion production, Physical Review C **82**, 065202 (2010).

[65] S. V. Mikhailov and N. G. Stefanis, Pion transition form factor at the two-loop level vis-a-vis experimental data, Mod. Phys. Lett. A **24**, 2858 (2009), arXiv:0910.3498 [hep-ph].

[66] A. P. Bakulev, S. V. Mikhailov, A. V. Pimikov, and N. G. Stefanis, Pion-photon transition: The New QCD frontier, Phys. Rev. D **84**, 034014 (2011), arXiv:1105.2753 [hep-ph].

[67] X.-G. Wu and T. Huang, Constraints on the Light Pseudoscalar Meson Distribution Amplitudes from Their Meson-Photon Transition Form Factors, Phys. Rev. D **84**, 074011 (2011), arXiv:1106.4365 [hep-ph].

[68] S. J. Brodsky, F.-G. Cao, and G. F. de Teramond, Evolved QCD predictions for the meson-photon transition form factors, Phys. Rev. D **84**, 033001 (2011), arXiv:1104.3364 [hep-ph].

[69] M. V. Polyakov, On the Pion Distribution Amplitude Shape, JETP Lett. **90**, 228 (2009), arXiv:0906.0538 [hep-ph].

[70] X.-G. Wu and T. Huang, An Implication on the Pion Distribution Amplitude from the Pion-Photon Transition Form Factor with the New BABAR Data, Phys. Rev. D **82**, 034024 (2010), arXiv:1005.3359 [hep-ph].

[71] P. Kroll, The form factors for the photon to pseudoscalar meson transitions - an update, Eur. Phys. J. C **71**, 1623 (2011), arXiv:1012.3542 [hep-ph].

[72] E. Ruiz Arriola and W. Broniowski, Pion transition form factor in the Regge approach and incomplete vector-meson dominance, Phys. Rev. D **81**, 094021 (2010), arXiv:1004.0837 [hep-ph].

[73] S. S. Agaev, V. M. Braun, N. Offen, and F. A. Porkert, Light Cone Sum Rules for the pi0-gamma*-gamma Form Factor Revisited, Phys. Rev. D **83**, 054020 (2011), arXiv:1012.4671 [hep-ph].

[74] M. Gorchtein, P. Guo, and A. P. Szczepaniak, Form factors of pseudoscalar mesons, Phys. Rev. C **86**, 015205 (2012), arXiv:1102.5558 [nucl-th].

[75] C. F. Redmer, Measurements of hadronic and transition form factors at besiii, in *EPJ Web of Conferences*, Vol. 212 (EDP Sciences, 2019) p. 04004.

[76] R. L. Workman *et al.* (Particle Data Group), Review of Particle Physics, PTEP **2022**, 083C01 (2022).